Received: 2 May 2019 | Revised: 29 July 2019 | Accepted: 31 July 2019

DOI: 10.1002/er.4832

RESEARCH ARTICLE

WILEY INTERNATIONAL JOURNAL OF ENERGY RESEARCH

# Thermal performance study of a vacuum integrated solar storage collector (ISSC) with compound parabolic concentrator (CPC)

**Anis Messaouda[1] | Majdi Hazami[1] | Farah Mehdaoui[1] | Mohamed Hamdi[2] | Marco Noro[3] | Renato Lazzarin[3] | AmenAllah Guizani[1]**

[1] Thermal Process Laboratory, Research and Technology Center of Energy, Borj-Cedria, Tunisia

[2] Laboratory of Wind Power Control and Waste Energy Recovery, Research and Technology Center of Energy CRTEn, Borj-Cedria, Tunisia

[3] Department of Management and Engineering, University of Padua, Vicenza, Italy

**Correspondence**
Anis Messaouda, Thermal Process Laboratory, Research and Technology Center of Energy, Borj-Cedria, Box 95 Hammam-Lif 2050, Tunisia.
Email: anismessaouda22@gmail.com

**Summary**

This paper deals with the energy performance of a new integrated solar storage collector (ISSC) with compound parabolic concentrator (CPC) conceived in the Thermal Process Laboratory in CRTEn Borj Cedria (North of Tunisia). The novelty in this system is the use of transparent vacuum insulation in the annulus between double half-Cylindrical Plexiglass, and the use of automated nocturnal insulation system, which suppresses heat loss during night. Also, the system is equipped with a mobile support permitting to have many collector orientations toward south, east-south, and west-south in order to maximize the incident solar flux. The experimental study of the ISSC system showed that the thermal loss coefficient of ISSC system is equal to 6.16 W/K for ISSC without nocturnal insulation and without vacuum, 4.69W/K for ISSC without nocturnal insulation and with vacuum, and 4.00 W/K for ISSC with nocturnal insulation and with vacuum. The thermal efficiency of the solar collector is equal to 42.92% for ISSC system fixed without vacuum, 45.95% for ISSC system fixed with vacuum, and 50.56% for ISSC system mobile with vacuum. In order to determine the long-term performance of the vacuum ISSC with CPC, the TRNSYS simulations were carried out by using the component modules modeling the ISSC with CPC concentrator (type 74 and type 60f). Comparison between experimental and predicted results for the temperature difference inside the storage tank during 3 days of January showed reasonable agreement. The numerical results for the ISSC system showed that the annual total energy

**Nomenclature:** $A_c$, collector area, $m^2$; $C_p$, specific heat of water at constant pressure, J/(kgK); $F_R$, overall collector heat removal efficiency factor, −; $F'$, collector fin efficiency factor, −; $H$, irradiation on tilted surface of the system, $MJ/m^2$; $I_{b_{ti}}$, instantaneous beam irradiation intensity on tilted surface, $W/m^2$; $I_{d_{ti}}$, instantaneous diffuse irradiation intensity on tilted surface, $W/m^2$; $I_{T_{ti}}$, instantaneous irradiation intensity on tilted surface, $W/m^2$; $I_{bT}$, beam radiation incident on the solar collector, $kJ/(hm^2)$; $I_{dT}$, diffuse horizontal radiation, $kJ/(hm^2)$; $I_T$, global radiation incident on the solar collector, $kJ/(hm^2)$; $Q_u$, useful energy supplied by the system, MJ; $U_L$, overall thermal loss coefficient of the collector per unit area, $kJ/(hm^2K)$; $U_s$, loss coefficient of the system, W/K; $T_a$, ambient temperature, °C; $T_{a_{av}}$, average ambient temperature during test, °C; $T_i$, inlet temperature of fluid to collector, °C; $T_O$, outlet temperature of fluid to collector, °C; $T_f$, final temperature of heating, °C; $T_{in}$, initial temperature of heating, °C; $V_s$, volume of the storage tank, $m^3$; $\Delta t$, cooling period, s; $\rho$, average water density, $kg/m^3$; $\eta_J$, daily thermal efficiency, %; $\alpha$, short-wave absorptance of the absorber plate, −; $\tau$, short-wave transmittance of the collector cover, −; $(\tau\alpha)$, product of the cover transmittance and the absorber absorptance, −; $(\tau\alpha)_b$, $(\tau\alpha)$for beam radiation, −; $(\tau\alpha)_d$, $(\tau\alpha)$for diffuse radiation, −

  

collected (solar) and auxiliary energy were about 4670 and 1561 MJ, respectively. The annual total auxiliary energy represents about 33.4% of the annual total energy collected (solar). During the summer months (June, July, and August), no auxiliary is needed and the solar fraction (SF) is equal to 100%, where as the annual average SF is about 75%.

**KEYWORDS**

CPC, experiments, ISSC, simulation, solar water heating, vacuum, thermal performance, TRNSYS

## 1 | INTRODUCTION

With oil prices soaring and the problems of pollution and global warming, research in the field of solar energy is attracting growing interest. Given the role it can play in countries like Tunisia, receiving a relatively high annual exposure of approximately 3000 hours of sunshine and an average daily global radiation of 5 kWh/m$^2$,[1] solar energy appears promising for the future valuable for energy saving. This energy can be used effectively for domestic hot water (DHW), building heating, and desalination. The rapid development of modern methods of using solar energy has led to the development of several types of solar water heating systems.

In general, a great interest was given to the exploitation of DHW systems with flat plate collector (FPC) in order to cover households' needs. However, the investment cost of the FPC DHW system is until today high compared with gas/gas town water heater system, which is economically nonsuitable. Besides, the FPC DHW system is quite complicated and demand more manufacturing effort as the solar collector and a storage tank are installed separately. To overcome this inconvenience, many studies are oriented to improve thermal performances of ISSC systems.

In order to evaluate the potential benefits of using ISSC technology in solar water heating and to improve their thermal efficiencies, several experimental and numerical studies appeared. The first restriction of ISSC is the thermal losses at night caused by reversal flow. To reduce its nighttime losses, the front of the ISSC system must be covered during the night. To remove these defects, different approaches have been explored to minimize heat loss in the system by conduction, convection, and infrared radiation, while encouraging the transmission of infrared radiation between visible and near-ambient and within the system.[2] For that, several solutions have been adapted. One of these solutions is insulation performed by the front face with a double glazing, which can avoid transfer by conduction and convection.[3] Low-emissivity coatings can be used to reduce radiative heat transfer. However, this technique requires the good performance of the transparent cover to the pressure difference between both sides. In the case of glass, this condition is satisfied with a cylindrical shape (thermos). But in the case of flat surfaces, it is necessary to use carriers, which then induce convective exchanges. In order to reduce thermal radiation heat transfer between surfaces, it is also necessary to provide a perfect insulation, which is difficult to achieve in practice. Berthou et al,[4] Rommel and Wagner,[5] and Schmide et al[6] used transparent insulation materials (TIMs) in improved solar water flat plate and integrated collector storage.

An ISSC system with compound parabolic concentrating reflectors is investigated experimentally by Helal et al.[7] The obtained thermal performances are compared with two other systems (STS-1 and STS-2) of solar water, proposed by Tripanagnostopoulos and Souliotis,[8] and which consist of single horizontal cylindrical water storage tanks placed in symmetrical and asymmetrical CPC reflectors. The results show that the thermal loss coefficient per aperture area (in W/(Km$^2$)) varies between 3.7 and 3.9 for ISSC system, 5 and 5.36 for STS-1 and 5.4 and 5.69 for STS-2.Varghese et al[9] conducted a parametric study of a new concentrating integral solar storage water heater. Unlike conventional CPC systems with a large number of smaller diameter tubes, they used a single larger diameter drum at the focus of the CPC. Their system used an air gap at the arms of the CPC. The results showed that the system has a maximum thermal efficiency of 38 %. A new type of CPC solar air collector with flat micro-heat pipe arrays (FMHPA) was studied by Zhu et al.[10] A cylindrical absorber was conceived by introducing the FMHPA into an evacuated glass tube to evacuate heat during the functioning process. Experimental tests were accomplished by the authors, in order to study the thermal efficiencies and the thermal heat loss coefficients of the new collector. In their review paper, Souliotis et al[11] presented different concentrating and non-concentrating Integrated Collector Storage systems. They also compared between different ICS geometries and strategies used to reduce heat losses. They found that the concentrating ISSC type shows better efficiency at low cost, but it suffers from night/overcast sky condition.

Their study shows that including phase change material (PCM) improves the water temperature capacity. They also concluded that more studies are still needed to reduce nighttime heat losses. Tadahmun et al[12] investigated experimentally the performance of an integrated solar water heater with corrugated absorber surface. They studied the system with and without flow rate. Without flow rate, their results showed an increase of the stored water temperature compared with the previous works. They also obtained a daily thermal efficiency of 67% when they used a mass flow rate 0.013 kg/s. Smyth et al[13] conceived and studied a hybrid photovoltaic (PV)/solar thermal system, which is compatible with traditional façade structures. Their results showed that heat retention efficiencies of the system were 8.3%, 23.6%, and 28% when they used unglazed, single transparent cover and double-glazed unit, respectively.

Several mathematical models have been proposed in open literature to simulate solar systems with a CPC by varying the parameters according to their studies. Hadjiat et al[14] used a system consisting of a storage tank (absorber) and a transparent cover placed on the front face. Fraidenraich et al[15] used a tube as absorber element, Tchinda et al[16] used a tube surrounded by a glass envelope, whereas Farouk et al[17] used the vacuum tube as absorbing element. Antonelli et al[18] proposed a methodology to estimate thermal heat losses inside compound parabolic concentrator (CPCs) to be used in designing of a new concept of solar collectors. In their work, CFD simulations were carried out on different CPCs, taking into account the effective working conditions and the presence of radiative heat transfer. The results obtained were used to develop some correlations by interpolation of numerical data, in order to evaluate the heat losses of the receiver and to illustrate the influence of different parameters such as the shape of receiver, tilt angle, and concentration ratio on the CPC solar collector efficiency. The performance of a prism-shaped storage solar collector with a right triangular cross-sectional area was investigated numerically by Joudi et al.[19] The ANSYS software release 5.4 was used for this purpose. Modifications were introduced embodying water properties and making the software compatible with the different types of loads. The results of this study have shown that the mean tank temperature reached was 37°C in 1 January and 46°C in 21 June without partition, with a good agreement with the theoretical and experimental results available in the literature. From their part, Wang et al[20] studied the performances of CPCs with tubular absorbers and without tracking system. They showed that reducing the gap loss is important for utilization of the concentrators. Wang et al proposed a detailed numerical model to evaluate the optical efficiency of a CPC solar collector conceived and realized in their laboratory. They found that the optical efficiency is divided into the beam and diffuses optical efficiency. Hadjiat et al[21] presented a new design of integrated collector storage solar water heater combined with CPC. The new configuration of the ISSC system consists of one cylindrical tank properly mounted in a stationary symmetrical CPC reflector. In this work, the authors studied the optical efficiency of the integrated collector storage solar water heater by using advanced ray tracing technique. They showed that the acceptance angle is about 40°. Harmim et al[22] studied experimentally and numerically the performance of a new design of an ISSC system equipped with a linear parabolic reflector. Their results showed that the system is effective only in winter. In particular, with an initial temperature of 22°C, the output temperature of the system reached 49°C.

As a matter of fact, reducing thermal loss coefficient, maximizing solar incident irradiation and so improving thermal performance of the ISSC systems are areas of further research works. In this study, we conduct an experimental and numerical investigation of an ISSC with vacuum and CPC (Figure 1). We focus on improving the thermal efficiency, expanding the field of use, and meet the criteria of cost reducing to make water heating affordable for the Tunisian home while ensuring an acceptable level of performance. The key innovation in this system is the use of a vacuum between the double glazing, which avoids heat transfer by conduction and convection between the storage tank and the ambient air. This technique was classically used in the vacuum solar collectors, but it usually presents practical problems in the ICS systems. This is due to the fact that building the vacuum between the absorber and the flat transparent insulation is difficult to achieve. In this study, this drawback is faced by using double half-cylindrical transparent insulation plexiglass (Figure 2). Also, we use an automated insulation system, which suppresses heat loss during night (Figure 3). The ISSC system is equipped with a mobile support allowing having many collector orientations toward south, east-south, and west-south in order to maximize the incident solar flux (Figure 4). The experimental study was essentially based on the evaluation of the effect of the vacuum and the night insulation on thermal performances, ie, the thermal loss coefficient and the thermal efficiency of the system. The numerical study was accomplished with TRNSYS simulation program by considering the Tunisian scenario. The TRNSYS program was used to simulate the long-term performance, the energy supplied by system during the entire year, the monthly/yearly needs of the auxiliary energy, and the solar fraction (SF) of the ISSC system.

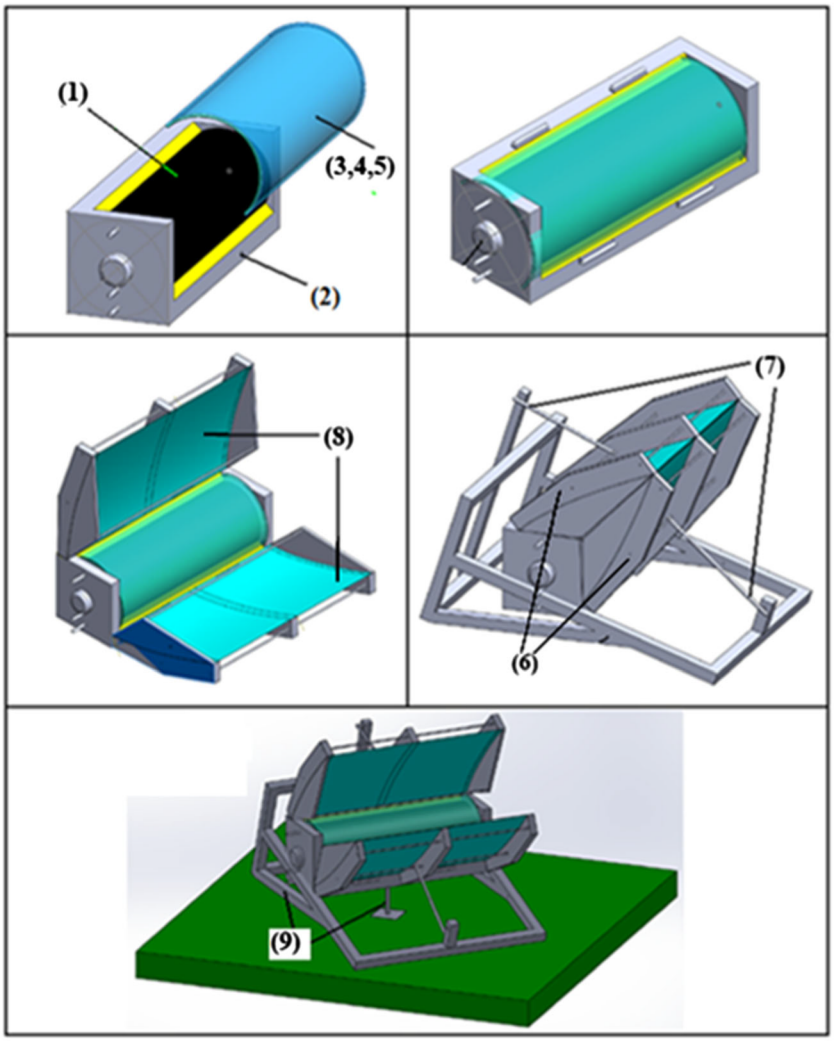


**FIGURE 1** Schematic view of vacuum integrated solar storage collector with vacuum integrated solar storage collector [Colour figure can be viewed at wileyonlinelibrary.com]

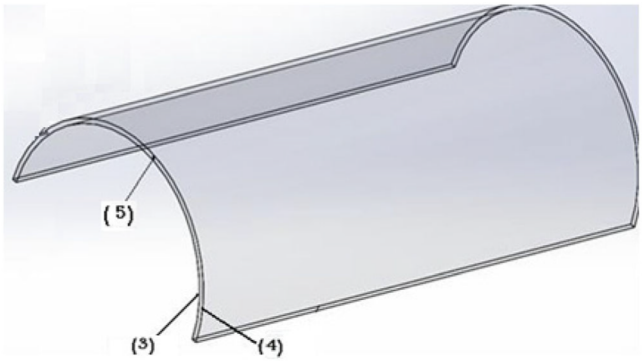


**FIGURE 2** The double Plexiglas transparent insulation with vacuum [Colour figure can be viewed at wileyonlinelibrary.com]

## 2 | EXPERIMENTAL INVESTIGATION

### 2.1 | System description

In Figure 1, the vacuum ISSC with CPC, which was designed and manufactured in the LPT laboratory in CRTEn, is presented. The aperture area of the conceived ISSC system is about equal to 0.85 $m^2$.It mainly consists of a cylindrical storage tank (1) with a storage capacity of 200 L, a diameter equal to 0.42 m, and a length equal to 1.45 m. The cylindrical storage tank, which represents the absorber element of the system, is partially painted in black paint and exposed to the Sun. The other part of the storage tank has a thermally insulated lower part of 30 mm of thickness made with polyurethane foam (2). The thermal conductivity of the polyurethane foam is about 0.32 W/(mK), and its specific heat is equal to 2090 J/(kgK). The main role of the polyurethane foam is the insulation of the underneath of the ISSC system and so the reduction of the thermal losses due to the conduction through the lower part of the system. The part of the tank surface exposed to the Sun is insulated using a double Plexiglas transparent insulation (3,4) in which we created a vacuum (5) (Figure 2). The role of the double Plexiglass insulation is to avoid escaping the radiation emitted by the absorber through the glass, which increases the water temperature. The two aluminum dish slices are covered

**FIGURE 3** The automated nocturnal insulation [Colour figure can be viewed at wileyonlinelibrary.com]


**FIGURE 4** Integrated solar storage collector system orientations toward south, east-south, and west-south (a mobile support) [Colour figure can be viewed at wileyonlinelibrary.com]

by an Armaflex insulation (6) and have two electric cylinders (7), which are connected to the trunk in order to perform the night insulation system and the CPC (8). The CPC has an acceptance half angle $\beta = 37.46°$ and a concentration ratio $C = 1/\sin\beta = 1.64$[28]. The assembly is carried on a movable support (9) allowing having many collector orientations toward south, east-south, and west-south in order to maximize the incident solar flux.

Technical specifications of the components of the ISSC system are summarized in Table 1, and the CPC geometric characteristics are given in Figure 5.

## 2.2 | Experimental framework

To investigate the thermal performance of the system at different climatic conditions, a framework testing protocol (Figure 6) was employed. The ISSC system was mounted in CRTEn Borj-Cedria (North of Tunisia) with latitude of 36.50°N, a longitude of 10.44°E on the stand-oriented E-W and a tilted angle of 45° towards the south.

**TABLE 1** Technical specification of the ISSC system components

| Element | Characteristics |
|---|---|
| Storage tank (Absorber) | Stainless steel<br>Black paint (absorption coefficient = 0.94)<br>Volume: 200 L<br>Length: 1.45 m<br>Diameter: 0.42 m |
| Box of the tank | Length: 1.55 m<br>Width: 0.50 m<br>Height: 0.50 m<br>Collector area: 0.85 $m^2$ |
| Back insulation | Injected polyurethane foam<br>Density: 30 $kg/m^3$<br>Average thickness: 40 mm |
| Transparent insulation (Plex1and Plex2) | Plexi glass (transmission coefficient 0.85)<br>Thickness: 4 mm<br>Diameter 1: 0.50-m diameter 2: 0.52 m |
| CPC reflector | Aluminum (reflection coefficient 0.9)<br>Acceptance angle: $2\beta = 2\times37.46 = 74.92°$)<br>Concentration ratio ($C = 1/\sin\beta = 1.64$) |

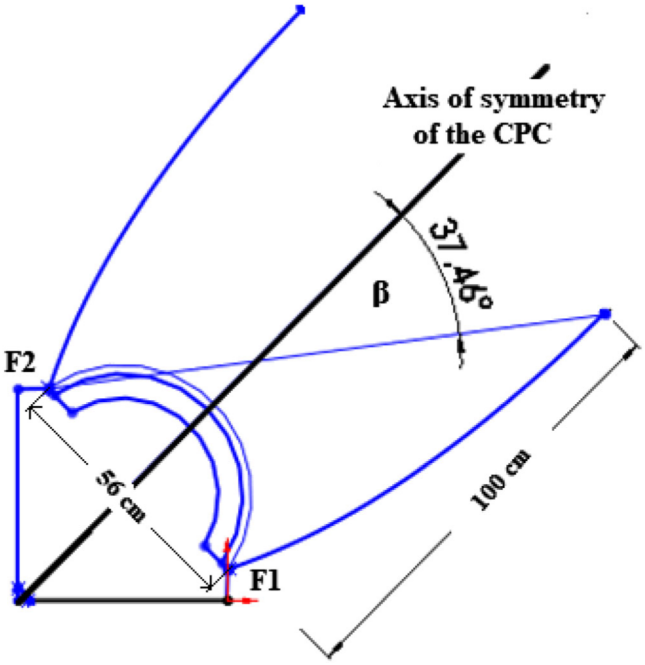


**FIGURE 5** Geometry for the compound parabolic concentrator (CPC reflector) [Colour figure can be viewed at wileyonlinelibrary.com]

Physical measurement parameters include ambient temperature ($T_a$) and water temperatures at the inlet and the outlet ($T_i$, $T_o$) of collector by using Platinum temperature sensors (Pt100) placed at two specific positions. All Pt100 sensors were firstly calibrated to an absolute measuring error less than 0.1°C and a relative deviation between each other less than 0.05°C. A flow meter was integrated to the collector experimental device to evaluate the water mass flow rates during every experience. A pyranometer (Kipp&Zonen) (10) with the measuring error less than 1% was installed close to the system experimental device to follow the incident solar irradiation changes. A multichannel digital data acquisition unit (type HP34970A Agilent) (11) was connected to the ISSC system experimental device to collect the data obtained during the measurements. In order to trait the collected data, the multichannel acquisition unit was connected to a computer (12) equipped with HP-VEE software.

## 2.3 | Uncertainty analysis

An uncertainty analysis was also achieved in order to appraise the precision of the experiments achieved in the laboratory. The investigation showed that the measurement errors were mainly attributed to the uncertainty of the experimental framework and measurement equipment (Table 2).

- Errors of the experimental framework: it was also seen that the errors occurring during measurement were about ±0.25 %.
- Errors of the measurement apparatus: it was found that the sensitiveness of data acquisition system and the Pt100 temperature sensor were about ±0.15%, and ±0.15°C, respectively. The sensitiveness of the flow meter integrated in the ISSC system device was about ±0.15%.

In order to evaluate the effects of the uncertainty of the experimental framework and measurement equipment on the precision of the experimental results, another investigation was theoretically accomplished. The investigation was structured on the evaluation of the coefficient $F$ by using Equation 1. In this equation,

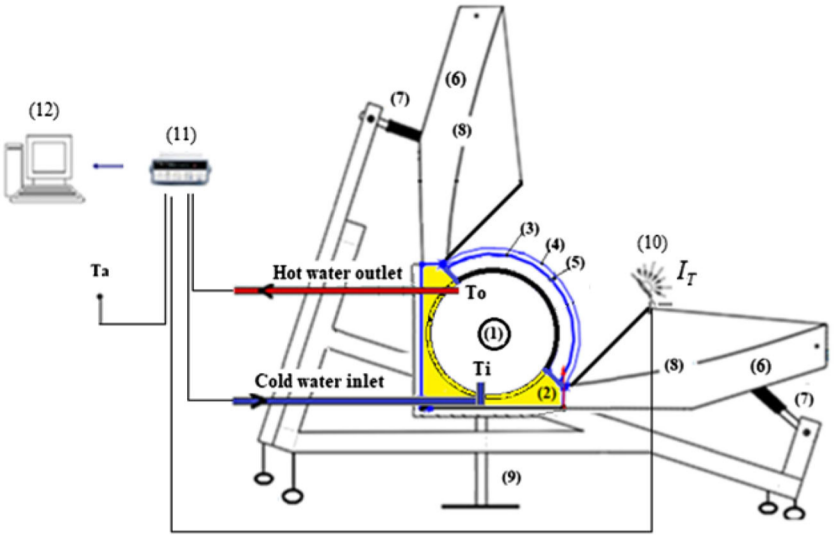


**FIGURE 6** Experimental device mounted for testing the integrated solar storage collector system [Colour figure can be viewed at wileyonlinelibrary.com]

**TABLE 2** Uncertainty of the sensors at typical test conditions

| Parameters | Units | Values |
|---|---|---|
| Water temperature | °C | ±0.05 |
| Ambient air temperature | °C | ±0.1 |
| Water mass flow | kg/s | ±0.25% |
| Solar irradiation | W/m$^2$ | ±0.1% |

$F$ represents the result obtained by the experimentation. The uncertainty of the results, $W_F$, was evaluated according to functioning parameters; $z_1$, $z_2$, .., $z_n$ and the independent variables uncertainties $w_1$, $w_2$, .., $w_n$.

$$w_F = \left( \left(\frac{\partial F}{\partial z_1} w_1\right)^2 + \left(\frac{\partial F}{\partial z_2} w_2\right)^2 + .... + \left(\frac{\partial F}{\partial z_i} w_i\right)^2 + ... + \left(\frac{\partial F}{\partial z_n} w_n\right)^2 \right)^{1/2}, \quad (1)$$

As an example we mention, the uncertainty estimation of the thermal energy (Equation 2). In Equation 2 $w_{\dot{m}}$, $w_{Qu}$, $w_{Cp}$, $w_{Tw}$, $w_{T_m}$, and $w_{I_r} w_G$ represent the measurements uncertainty of the hot water flow-rate, the useful energy, the specific heat, the hot water temperature, the ambient temperature, and the solar irradiation, respectively.

$$w_E = \left( \left(\frac{\partial E}{\partial \dot{m}} w_{\dot{m}}\right)^2 + \left(\frac{\partial E}{\partial Qu} w_{Qu}\right)^2 + \left(\frac{\partial E}{\partial C_p} w_{C_p}\right)^2 + \left(\frac{\partial E}{\partial T_w} w_{T_w}\right)^2 + \left(\frac{\partial E}{\partial T_m} w_{T_m}\right)^2 + \left(\frac{\partial E}{\partial I_T} w_{I_T}\right)^2 \right)^{1/2}. \quad (2)$$

The detailed results of the uncertainty parameters investigation are given in Table 3.

**TABLE 3** Evaluation of the parameters uncertainties

| Parameters | Symbol | Unit | Uncertainty |
|---|---|---|---|
| Hot water temperature | $T_w$ | °C | ±0.84 |
| Outlet hot water temperature | $T_O$ | °C | ±0.76 |
| Ambient temperature | $T_m$ | °C | ±0.61 |
| Useful collected energy | $E_U$ | W | ±2.51 |
| Energy efficiency | $\eta_{En}$ | % | ±1.64 |
| Heat losses coefficient | $U_l$ | W/K | ±0.08 |
| Solar fraction | $SF$ | % | ±1.15 |

# 3 | THERMAL PERFORMANCES OF THE ISSC SYSTEM

## 3.1 | Thermal loss coefficient

To enhance the thermal performances of the ISSC system, it is necessary to reduce at least the overall heat lost energy, $Q_l$ ($W$) (Equation 3) especially during the night.[23]

$$\mathrm{Q_l(W)} = U_s A_c \left(T_{\mathrm{abs,av}} - T_a\right). \quad (3)$$

In Equation 3, it was considered the heat exchange between the absorber and the ambient air. It is trivial that the rate of convective thermal loss energy increases with the increase of the temperature difference between the absorber and the ambient air ($T_{\mathrm{abs,\ av}}$- $T_a$). The measurement of the thermal loss coefficient $U_s$ of the ISSC system was evaluated by standard Tunisia (NT 67.10)[24]. This measurement step is performed according to this standard: filling the storage tank and heating to a temperature above 60°C, then placing the assembly in a room at a known temperature for 24 hours. The measurement of water temperatures at the initial state and final state allows the evaluation of the thermal loss coefficient by applying the following formula (Equation 4):[23]

$$U_s = \frac{\rho C_p V_s}{\Delta_t} Ln \frac{T_{in} - T_{a_{av}}}{T_f - T_{a_{av}}}. \quad (4)$$

Our experimental approach consists of three steps for determining the thermal loss coefficients of the ISSC system: without nocturnal insulation and without vacuum, without nocturnal insulation and with vacuum, and with nocturnal insulation and with vacuum.

In Table 4, the average value of the ambient temperature during the test period, the initial and final hot water temperatures, and the thermal loss coefficient for the three configurations of the ISSC system are reported. Note that for the ISSC system without nocturnal insulation and without the vacuum, the temperature of the hot water at the begin is equal to 68.5°C; after 24 hours, this temperature became equal to 48°C for an average ambient temperature of 26.75°C, which gives a loss coefficient equal to 6.16 W/K. It is also noted that the loss coefficient of ISSC system is reduced by about 23.86% when the vacuum between the two transparent insulations plex1 and plex2 is created; this is explained by the fact that the convective heat transfer is negligible in the vacuum. The table also shows that the coefficient of loss decreases further when using a nocturnal insulation (ISSC system with nocturnal insulation and with vacuum): in this case, it becomes equal to 4.00 W/K with a decrease of about 14.70% compared with that of the

**TABLE 4** Experimental conditions for determine the heat loss coefficient of different configurations of the ISSC system

| | ISSC System Without Nocturnal Insulation and Without Vacuum | ISSC System Without Nocturnal Insulation and With Vacuum | ISSC System With Nocturnal Insulation and With Vacuum |
|---|---|---|---|
| $T_a$, ° C | 26.75 | 26.38 | 24.82 |
| $T_i$, ° C | 68.5 | 70.5 | 69 |
| $T_f$, ° C | 48 | 53.5 | 54 |
| $\Delta t$,s | 86400 | 86400 | 86400 |
| $U_s$,W/K | 6.16 | 4.69 | 4.00 |

Abbreviation: ISSC: integrated solar storage collector.

ISSC system without nocturnal insulation and with vacuum (which is equal to 4.69 W/K), and of the order of 35% compared with that of the ISSC system without nocturnal insulation and without the vacuum. Finally, the ideal configuration for our system is the ISSC with nocturnal insulation and using vacuum between the two transparent Plexiglas insulations. When comparing our results with those of previous works published by Helal et al[7], Tripanagnostopoulos et al[8], Singh et al,[11]and Dharuman et al,[25] it is shown that the heat loss coefficient of the ISSC system varies between 2 and 7 W/K. It can be concluded that the system here proposed presents an acceptable heat loss coefficient compared with other similar ISSC systems given in the literature.

## 3.2 | Thermal efficiency

The second component of the thermal performance of the system is its daily output $\eta_J$. It is defined as the ratio of the useful energy ($Q_u$) to the irradiation energy on tilted surface ($H$) received by the system as the following:[26]

$$\eta_J = \frac{Q_u}{HA_c} \tag{5}$$

where $A_c$ is the collector area.

The evaluation of the daily output is obtained using the method of input/output,[26] which consists of filling up the storage tank with cold water at constant temperature and let it warm up by solar radiation for twelve hours. At the end of the day, we fill it with a volume of water equivalent to 3 times the volume of the storage balloon with a flow rate of 10 L/min.

To determine the useful energy ($Q_u$) and the irradiation on tilted surface ($H$) received by the system, the water temperatures at the inlet and outlet of the collector ($T_{ii}$, $T_{oi}$) are measured at time intervals of $t_1$=30 seconds, and the radiation intensity is measured throughout the day with a time step of $t_2$=300 seconds. These measures allow evaluating ($Q_u$) and ($H$) by applying Equations (6) and (7), respectively[26]:

$$Q_u = \dot{m} C_p t_1 \sum_{i=1}^{n} (T_{oi} - T_{ii}), \tag{6}$$

where $\dot{m}$ is themass flow rate (kg/s), $C_p$ is the average water specific heat (J/(kgK)), and $n$ is the number of withdrawal.

$$H = t_2 \sum_i I_{T_{ti}} = t_2 \sum_i I_{b_{ti}} + I_{d_{ti}}. \tag{7}$$

where $I_{T_{ti}}$ is the instantaneous irradiation intensity on tilted surface, $I_{b_{ti}}$ is the instantaneous beam irradiation intensity on tilted surface, and $I_{d_{ti}}$ is the instantaneous diffuse irradiation intensity on tilted surface in W/m$^2$.

The experimental approach consists of three steps for determining the thermal efficiency of the ISSC system fixed without vacuum (a), the ISSC system fixed with vacuum (b), and the ISSC system mobile with vacuum (c).

Figure 7 shows the evolution of the ambient temperature and the total irradiation on tilted surface for the 3 days of tests (a, b, and c). The days of 15 October 2017 (a) and 17 October 2017 (b) are characterized by a clear sky and strong irradiation on tilted surface with a single peak ($I_{T\max}$= 1100 W/m$^2$), and the ambient temperature is between 20 and 23°C. The day of 12 October 2017 (c) is characterized by a clear sky and strong irradiation on tilted surface with several peaks ($I_{T\max}$=1100 W/m$^2$), which are at the origin of the mobility of the system, and the ambient temperature is between 20 and 23°C.

Figure 8 reports the variation of the temperature of the water at the outlet of the solar water heater during the drawdown for the three configurations of the ISSC system (ISSC system fixed without vacuum -a-, ISSC system fixed with vacuum -b-, and mobile ISSC system with vacuum -c-). During the tests, a withdrawal rate of 10 L/min is adopted.

It can be noted that the temperature of the water at the outlet of the solar water heater decreases exponentially and tends towards the value of the temperature of the renewal water at the inlet of the solar water heater, which is of the order of 23°C. This decrease is even less rapid when the system is under vacuum and when it is mobile.

It is worth to note that the exit temperature during the day of 17 October 2017 (ISSC system fixed with the vacuum -b-) is higher than that relative to the day of 15 October 2017 (ISSC system fixed without the vacuum -a -).This is due to the decrease in convective thermal losses obtained by the creation of the vacuum. Moreover, the exit temperature during the day of 12 October 2017 (ISSC

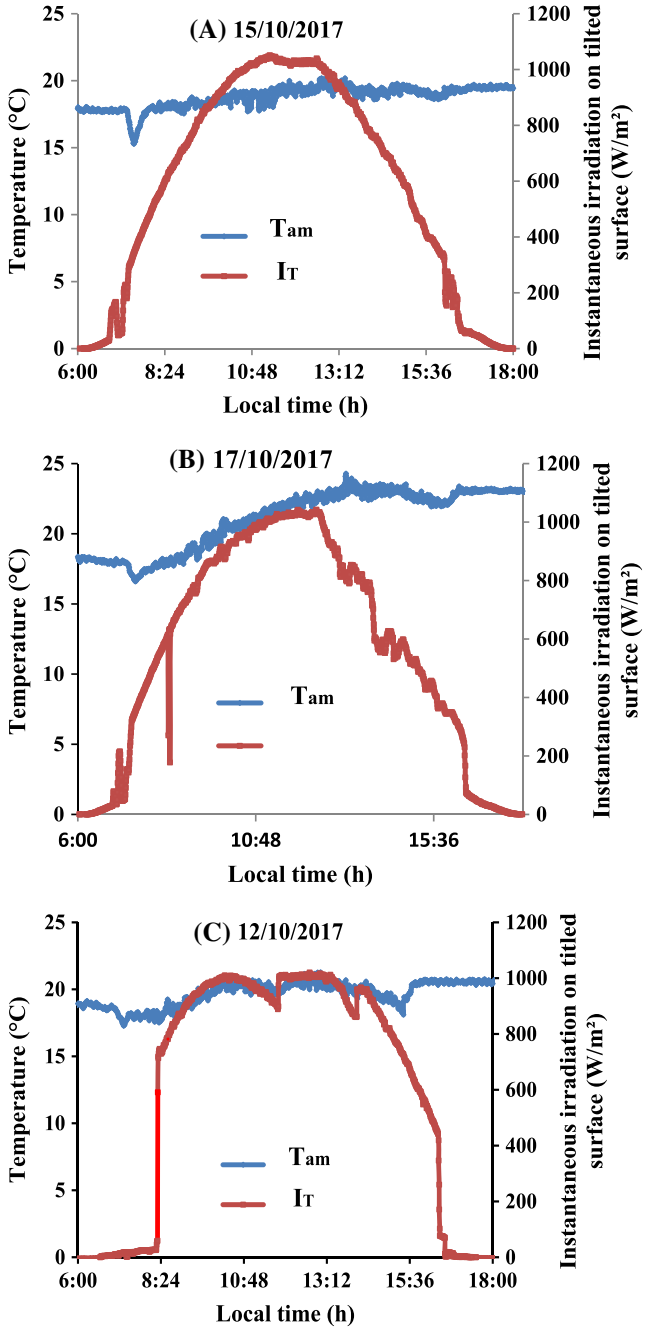


**FIGURE 7** Climatic data of the integrated solar storage collector system for three days and configurations (a), (b), and (c) [Colour figure can be viewed at wileyonlinelibrary.com]

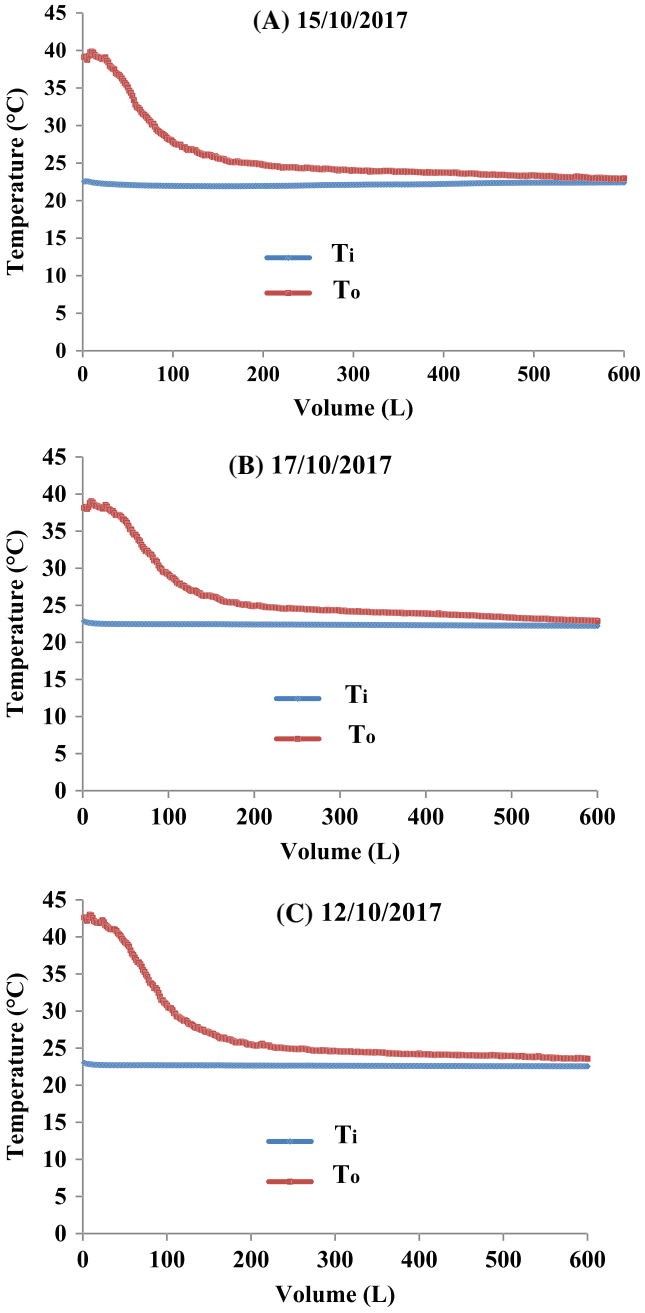


**FIGURE 8** Thermal profile of the integrated solar storage collector system for three days and configurations (a), (b), and (c) [Colour figure can be viewed at wileyonlinelibrary.com]

system mobile with the vacuum -c-) is higher than that relative to the days of 15 October 2017 (ISSC system fixed without the vacuum -a-) and 17 October 2017 (ISSC system fixed with vacuum -b-); this is due to the excess of energy received by the system during its tracking the Sun. The results also show that the amount of hot water withdrawn at an average temperature of 35°C during the day 17 October 2017 (ISSC system fixed with the vacuum -b-), which is of the order of 100 L, is more important than that relating to the day of 15 October 2017 (ISSC system fixed without the vacuum -a-), which is of the order of 80 L. Furthermore, it can be noted that the temperature of a quantity of 100 L of hot water withdrawn during the day of 12 October 2017 (ISSC system mobile with the vacuum -c-), which is of the order of 38°C, is more important than that of the day 17 October 2017 (ISSC system fixed with the vacuum -b-), which is of the order of 35°C.

In Table 5, it is shown the solar useful energy supplied ($Q_u$), the irradiation on tilted surface ($H$), and the daily thermal efficiency $\eta_J$ for the three configurations of the

**TABLE 5** Experimental conditions for determine the thermal efficiency of different configurations of ISSC system

| | ISSC System Fixed Without Vacuum | ISSC System Fixed With Vacuum | ISSC System Mobile With Vacuum |
|---|---|---|---|
| Test day | 15 October 2017 | 17 October 2017 | 12 October 2017 |
| $Q_u$, MJ | 9.21 | 9.45 | 11.27 |
| $H$, MJ/m$^2$ | 25.24 | 24.19 | 26.22 |
| $\eta_J$ , % | 42.92 | 45.95 | 50.56 |

Abbreviation: ISSC: integrated solar storage collector.

ISSC system during the 3 days of testing. Note that for the ISSC system fixed without the vacuum -a-, the energy supplied is of the order of 9.21 MJ for incident energy equal to 25.24 MJ/m$^2$, which gives a daily efficiency equal to 42.92%. This table also shows that the daily thermal efficiency of ISSC system fixed with the vacuum -b-, which is of the order of 45.95%, is higher by 10.9% compared with that of the system -a-. Hence, the importance of using vacuum between the two transparent plex1 and plex2 insulations, which reduces heat loss by convection, is demonstrated. Finally, the daily thermal efficiency of the ISSC system mobile with the vacuum, which is equal to 50.56%, increased by 9% compared with that of the ISSC system fixed with the vacuum and by 19% compared with that of the ISSC system fixed without the vacuum. These results show the importance of using a tracking system that increases the amount of energy received by the system and therefore increases the thermal efficiency. By consulting literature, it was found that the ISSC system efficiency investigated by Varghese et al,[9] Tadahmun et al,[12] Smythet al,[13] Kessentiniet al,[27] and Chaurasia et al[28] is in the range from 38 to 60%. It can be concluded that the ISSC system we developed presents a good efficiency compared with other similar ISSC systems.

## 4 | LONG-TERM PERFORMANCES OF ISSC SYSTEM WITH VACUUM CPC CONCENTRATOR

The long-term performance of the ISSC with Vacuum and CPC concentrator was evaluated by using TRNSYS simulation program.[29] The TRNSYS program was used to simulate the monthly/yearly energy requests of a Tunisian household, the SF, and the energy supplied by the system during one year.

Although flat plate collectors are well studied and reviewed in the literature, there is still a lack of a complete and efficient model in TRNSYS able to predict the thermal behavior of ICS, and further research work is still needed. It is important to note that such a model could be incorporated in the modeling environment of TRNSYS. For modeling the ISSC system, the simulations were carried out by means of the component modules (type 74 and type 60f) and the circulating pump (type 114). Utilities have also been used: the meteorological data reader (type 109), the integrator (type 24), the results plotter (type 65), and the results printer (type 25c) (Figure 9). Many input parameters, such as ambient temperature, solar irradiation, and solar collector orientation, were analyzed to evaluate the thermal energy needs by considering a real Tunisian scenario.

During the TRNSYS program simulation, a DHW request profile of a typical Tunisian family composed of four persons was considered, which consists of a daily consumption of 200 L of hot water at a temperature equal to 40°C (Figure 10).

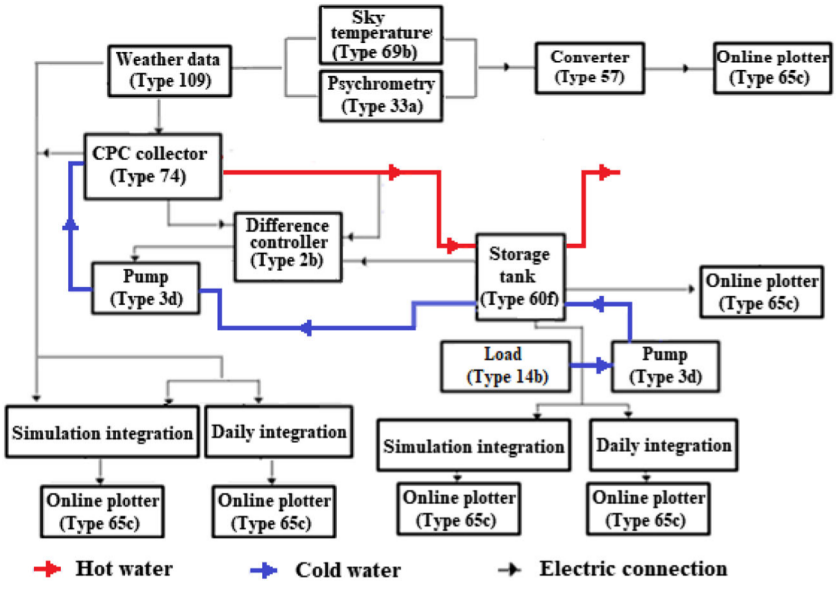


**FIGURE 9** Simulation diagram on TRNSYS program [Colour figure can be viewed at wileyonlinelibrary.com]

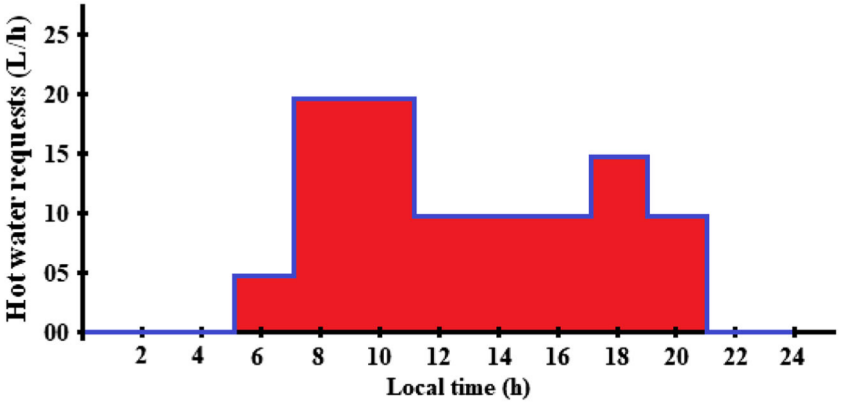


**FIGURE 10** Daily domestic hot water request of a typical Tunisian family consuming 200 l/day [Colour figure can be viewed at wileyonlinelibrary.com]

## 4.1 | Mathematical description of the Type 74 (CPC)

The useful energy by the CPC is modeled using the Hottel-Whillier collector equation (Equation (8)):[30]

$$Q_u = A_c F_R (I_T(\tau\alpha) - U_L(T_i - T_a)), \quad (8)$$

where *FR* is the overall collector heat removal efficiency factor given by the following Equation (9):29

$$F_R = \frac{mC_p}{A_c U_L}\left(1 - \exp\left(-\frac{F' U_L A_c}{mC_p}\right)\right). \quad (9)$$

The overall transmittance-absorbance product is calculated as (Equation 10) 29

$$(\tau\alpha) = \frac{I_{bT}(\tau\alpha)_b + I_{dT}(\tau\alpha)_d}{I_T} \quad (10)$$

## 4.2 | Validation of the TRNSYS simulation program

Figure 11 represents the variations of the experimental and simulated temperature difference in the ISSC system inside the storage tank during 3 days of January (when energy needs are high). A good according between measured and simulated values is reported, and the difference is in the range of 0–2.4°C. A comparison between experimental and numerical results of obtained thermal efficiencies of the ISSC system is reported in Table 6: a thermal efficiency of about 50.56% and 53.15 % are obtained experimentally and numerically, respectively. This trend of the results shows the accuracy of the proposed TRNSYS model.

Hence, we conclude that the TRNSYS simulation program could reproduce with an acceptable accuracy the real behavior of the ISSC system.

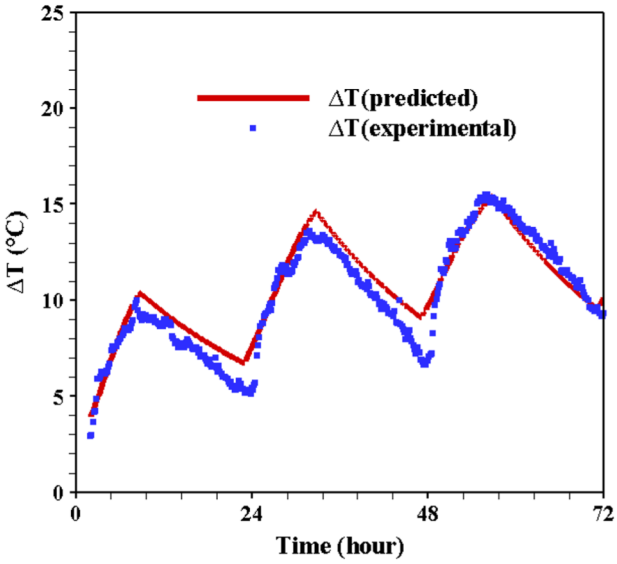


**FIGURE 11** Numerical and experimental temperature difference [Colour figure can be viewed at wileyonlinelibrary.com]

**TABLE 6** Experimental and numerical thermal efficiency of ISSC system

| | Experimental | Numerical |
|---|---|---|
| $Q_u$, MJ | 11.27 | 10.93 |
| $H$, MJ/m$^2$ | 26.22 | 24.20 |
| $\eta_J$, % | 50.56 | 53.15 |

## 4.3 | The ISSC system monthly and annual performances

Figure 12 represents the variations of the monthly average ambient temperature and solar irradiation on tilted surface. The former ranges between 27°C in August and 11.5°C in January, the latter ranges between 455 and 721 MJ/m$^2$. As can be noticed, the monthly average irradiation on tilted surface and ambient temperature present a similar profile. The annual average temperature and

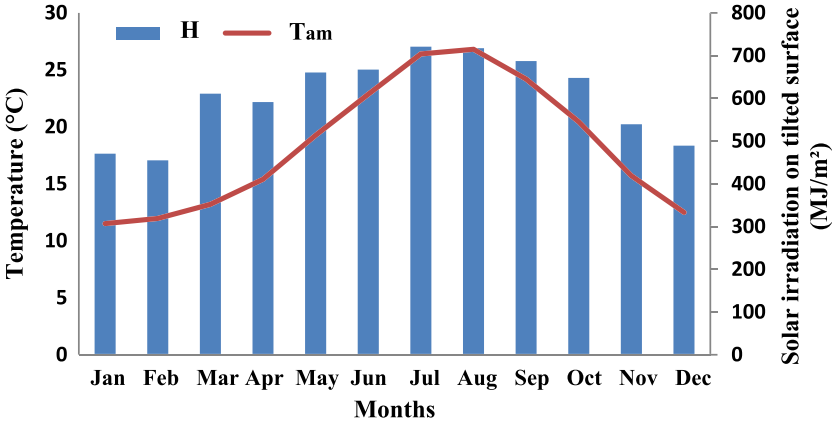


**FIGURE 12** Variations of the monthly average ambient temperature and solar irradiation on tilted surface [Colour figure can be viewed at wileyonlinelibrary.com]

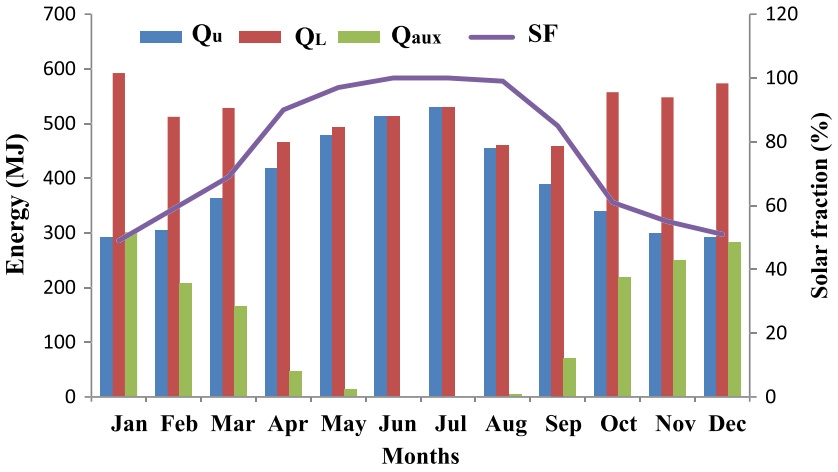


**FIGURE 13** Integrated solar storage collector system monthly energy flows and solar fraction variation [Colour figure can be viewed at wileyonlinelibrary.com]

irradiation on tilted surface reached in the site are 18.35° C and 604.3 MJ/m$^2$, respectively (Table 5).

Figure 13 reports the simulation of the solar useful energy supplied ($Q_u$), the auxiliary energy ($Q_{aux}$), the loaded energy ($Q_L$), and the SF changes.[31] The changes of *SF* are given by Equation 11:[32]

$$SF = 1 - Q_{aux}/Q_L. \quad (11)$$

The highest requests for DHW are noted for the period from October to March, which coincides with a shortage of solar irradiation. During this period, the loaded energy ranges between 512 and 592.4 MJ, while the useful thermal solar energy from the ISSC system ranges between 291 to 339 MJ. It was also found that from October to March, the ISSC system provides from 49 to 61% of the total DHW needs by considering merely solar energy (*SF*). Figure 13 implies also that *SF* is lower during the winter months, from October to March, and higher during the hot months (from April to September). It was found that during the hot months of the year, the loaded energy passes from 458.9 to 530 MJ with a SF ranging between 85% in September and 100% in June and July.

On a yearly basis, a rate of 6231 MJ of heat energy was loaded, 4670 MJ of solar thermal energy collected, and 1561 MJ of auxiliary energy requested, which give an annual average SF of about 75% (Table 7).

Another series of simulations was accomplished: Figure 14 illustrates the outlet temperature of fluid from ISSC system with and without auxiliary heating system. From May to August, there is no requisite of auxiliary heating system. This result confirms that the request of auxiliary energy is limited to the cold months of the year, chiefly from October to Mars.

Figure 14 shows that, without making appeal to the auxiliary heating system, the monthly average temperature of fluid exiting the **ISSC** system during cold months (from October to Mars) ranges between 30 and 40°C. When the auxiliary heating system is activated, the temperature ranges from 42 to 45°C during the same period. We perceive that the auxiliary energy allows the gain of about 12°C compared with the outlet temperature of fluid without using auxiliary heating system.

**TABLE 7** Energy analysis and monthly temperature

| Month | $H$, MJ/m$^2$ | $T_{am}$, °C | $Q_u$ (solar), MJ | $Q_l$ (load), MJ | $Q_{aux}$, MJ | SF, % |
|---|---|---|---|---|---|---|
| January | 470.57 | 11.51 | 291 | 592.4 | 301.4 | 49 |
| February | 455 | 11.96 | 304.1 | 512.3 | 208.2 | 59 |
| March | 611.11 | 13.20 | 362.9 | 528.5 | 165.6 | 69 |
| April | 591.46 | 15.40 | 418 | 465.1 | 47.1 | 90 |
| May | 660.62 | 19.26 | 478.7 | 492.9 | 14.2 | 97 |
| June | 667.38 | 22.86 | 513.5 | 513.5 | 0 | 100 |
| July | 721.09 | 26.40 | 530 | 530 | 0 | 100 |
| August | 717.39 | 26.81 | 454.5 | 459.2 | 4.7 | 99 |
| September | 687.35 | 24.19 | 388.1 | 458.9 | 70.8 | 85 |
| October | 647.83 | 20.45 | 339 | 557.3 | 218.3 | 61 |
| November | 539.45 | 15.71 | 299 | 548 | 249 | 55 |
| December | 489.43 | 12.50 | 291.5 | 573.6 | 282.1 | 51 |
| Annual | 7258.70 | - | 4670.4 | 6231.4 | 1561 | 75 |
| Average | 604.33 | 18.35 | 389.2 | 519.3 | 130.1 | 75 |

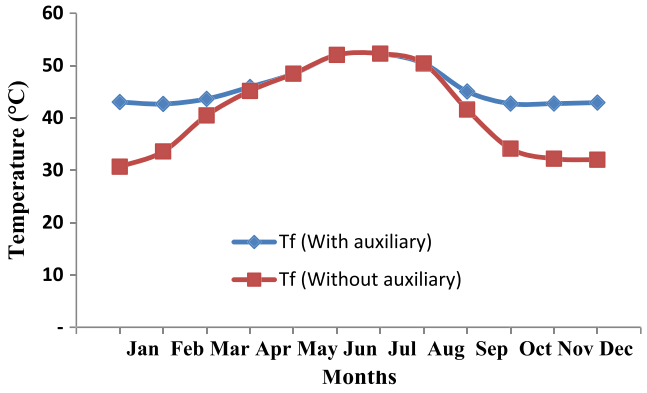


**FIGURE 14** Integrated solar storage collector water outlet temperature variation with and without auxiliary heating system [Colour figure can be viewed at wileyonlinelibrary.com]

## 5 | CONCLUSIONS

This work consists of the experimental and numerical study of a new ISSC system conceived in our laboratory. This study is intended as a contribution to the development of heliothermic applications, especially in Tunisia, and we firmly hope that this goal has been achieved. The main results of the thermal study of the system give the following conclusions:

1. The efficiency of the system is equal to 42.52, 45.95, and 50.56% for the ISSC system fixed without vacuum, ISSC system fixed with vacuum, and ISSC system mobile with vacuum, respectively.
2. The thermal loss coefficient is equal to 6.16, 4.69, and 4.00 W/K for the ISSC system without nocturnal insulation and without vacuum, ISSC system without nocturnal insulation and with vacuum, and ISSC system with nocturnal insulation and with vacuum, respectively.
3. A numerical model was developed by TRNSYS simulation in order to determine the long-term performance of the ISSC system.
4. Comparison of experimental data with predicted results for the temperature difference inside the storage tank during three days of January showed reasonable agreement.
5. The long-term performances of the ISSC system show that the annual average *SF* is about 75% for the annual total of energy collected and auxiliary energy, respectively, about 4670 and 1561 MJ.

The conclusion allows to open the following perspectives:

1. The association of the ISSC system with a natural gas booster system that will cover all the energy needs of a Tunisian family composed of four persons at lower cost.
2. The integration of PCM in the storage tank, which could improve the performance of the storage sensor and make it useful in other applications (in industrial sector, heating building, etc...).
3. Our ISSC system uses cylinders to achieve the night insulation that are operated by electricity. Actually, electric energy is generated at power plants, but it could be possible to operate the cylinders by PV solar panels. Then, the system can be self-sustainable in this case.
4. The ability of incorporating a new mathematical model into the commercial system modeling environment TRNSYS using FORTRAN remains to be studied and will make the object of our future work.

## ORCID

*Anis Messaouda* https://orcid.org/0000-0002-1920-1844
*Mohamed Hamdi* https://orcid.org/0000-0002-8867-2340

## References

1. Kerkeni C, Hamdi K, Dehmani L, Belghith A. Etude des performances thermiques à long terme d'un système solaire de chauffage de l'eau sanitaire. JITH. 1993:345-351.

2. Goetzberger A, Schmid J, Wittwer V. Transparent insulation system for passive solar utilization in buildings. 1st E.C. Conference on solar heating, Amsterdam, 1984.
3. Collins RE, Fischer-Cripps AC, Tang JZ. Transparent evacuated insulation. *Sol Energy*. 1992;49(5):333-350. https://doi.org/10.1016/0038-092X(92)90106-K
4. Berthou Y, Biwole PH, Achard P, Sallée H, Tantot-Neirac M, Jay F. Full scale experimentation on a new translucent passive solar wall combining silica aerogels and phase change materials. *Sol Energy*. 2015;115:733-742. https://doi.org/10.1016/j.solener.2015.03.038
5. Rommel M, Wagner A. Application of transparent insulation materials in improved flat-plate collectors and integrated collector storage. *Sol Energy*. 1992;49(5):371-380. https://doi.org/10.1016/0038-092X(92)90109-N
6. Schmide CH, Goetzberger A, Schmid J. Test results and evaluation of integrated collector storage systems with transparent insulation. *Sol Energy*. 1988;41(5):487-494. https://doi.org/10.1016/0038-092X(88)90022-9
7. Helal O, Chaouachi B, Gabsi S, Bouden C. Energetic performances study of an integrated collector storage solar water heater. *Am J Eng Appl Sci*. 2010;3(1):152-158. https://doi.org/10.3844/ajeassp.2010.152.158
8. Tripanagnostopoulos Y, Souliotis M. Integrated collector storage solar systems with asymmetric CPC reflectors. *Renew Energy*. 2004;29(2):223-248. https://doi.org/10.1016/S0960-1481(03)00195-2
9. Varghese J, Manjunath K. A parametric study of a concentrating integral storage solar water heater for domestic uses. *Appl Therm Eng*. 2017;111:734-744. https://doi.org/10.1016/j.applthermaleng.2016.09.127
10. Zhu TT, Diao YH, Zhao YH, Li FF. Thermal performance of a new CPC solar air collector with flat micro heat pipe arrays. *Appl Therm Eng*. 2016;101:479-489. https://doi.org/10.1016/j.applthermaleng.2015.12.033
11. Souliotis M, Singh R, Papaefthimiou S, Lazarus IJ, Andriosopoulos K. Integrated collector storage solar water heaters: survey and recent developments. *Energy Systems*. 2016;7(1):49-72.
12. Yassen TA, Mokhlif ND, Eleiwi MA. Performance investigation of an integrated solar water heater with corrugated absorber surface for domestic use. *Renew Energy*. 2019;138:852-860. https://doi.org/10.1016/j.renene.2019.01.114
13. Smyth M, Pugsley A, Hanna G, et al. Experimental performance characterisation of a hybrid photovoltaic/solar thermal façade module compared with a flat integrated collector storage solar water heater module. *Renew Energy*. 2018;237:137-143. https://doi.org/10.1016/j.renene.2018.04.017
14. Hadjiat MM, Bekkouche SMA, Zerga A, Benyoucef B, Yaichel MR. A new modeling approach of an ICS solar water heater with CPC reflectors. *Int J Energy Eng*. 2013;3(3):165-170. https://doi.org/10.5923/j.ijee.20130303.06
15. Fraidenraich N, De Lima R, Tiba C, Barbosa S. Simulation model of a CPC collectors with temperature-dependent heat loss coefficient. *Sol energy*. 1999;65(2):99-110. https://doi.org/10.1016/S0038-092X(98)00118-2
16. Tchinda R, Kaptouom E, Njomo D. Study of the C.P.C. collector thermal behaviour. *Energy Conver*. 1998;39(13):1395-1406. https://doi.org/10.1016/S0196-8904(97)10052-8
17. Farouk Kothdiwala A, Norton B, Eames PC. The effect of variation of angle of inclination on the performance of low-concentration-ratio compound parabolic concentrating solar collectors. *Sol energy*. 1995;55(4):301-309. https://doi.org/10.1016/0038-092X(95)00049-W
18. Antonelli M, Francesconi M, Di Marco P, Desideri U. Analysis of heat transfer in different CPC solar collectors: A CFD approach. *Appl Therm Eng*. 2016;101:479-489. https://doi.org/10.1016/j.applthermaleng.2015.12.033
19. Joudi KA, Hussein IA, Farhan AA. Computational model for a prism shaped storage solar collector with a right triangular cross section. *Energ Conver Manage*. 2004;45(3):391-409. https://doi.org/10.1016/S0196-8904(03)00153-5
20. Wang J, Yu L, Jiang C, Yang S, Liu T. Optical analysis of solar collector with new V shaped CPC. *Sol Energy*. 2016;135:780-785. https://doi.org/10.1016/j.solener.2016.06.019
21. Hadjiat MM, Ouali S, Gama A, Yaiche MR. Design and analysis of a novel ICS solar water heater with CPC reflectors. *J Energy Storage*. 2018;16:203-210. https://doi.org/10.1016/j.est.2018.01.012
22. Harmim A, Boukar M, Amara M, Haida AEK. Simulation and experimentation of an integrated collector storage solar water heater designed for integration into building façade. *Energy*. 2018;166:59-71. https://doi.org/10.1016/j.energy.2018.10.069
23. Tripanagnostopoulos Y, Souliotis M, Nousia T. CPC type integrated collector storage systems. *Sol Energy*. 2002;72(4):327-350. https://doi.org/10.1016/S0038-092X(02)00005-1
24. Teyeb A, Dehmani L, Ezzine AB, Kerkeni C, Kaabi L. Etude des performances thermiques d'un capteurstockeurcylindroparabolique. *Rev Energy Renew*. 2006;9:135-141.
25. Dharuman C, Arakeri JH, Srinivasan K. Performance evaluation of an integrated solar water heater as an option for building energy conservation. *Energ Buildings*. 2006;38(3):214-219. https://doi.org/10.1016/j.enbuild.2005.05.007
26. Jamel S. Test des chauffe-eau solaires, Validation de la méthode Input/Output. Projet de Fin d'Etudes, ENIT.2001.
27. Kessentini H, Bouden C. Numerical and experimental study of an integrated solar collector with CPC reflectors. *Renew Energy*. 2013;57:577-586. https://doi, https://doi.org/10.1016/j.renene.2013.02.015
28. Chaurasia PBL, Twidell J. Collector cum storage solar water heaters with and without transparent insulation material. *Sol Energy*. 2001;70(5):403-416. https://doi.org/10.1016/S0038-092X(00)00158-4
29. TRNSYS 17, Component Libraries for the TRNSYS Simulation Environment, Volume 3, "Standard Component Library Overview".
30. Solar Energy Laboratory. TRNSYS 17 mathematical reference. In: *Available under the TRNSYS 17 Help Menu*. Madison, WI, USA: Solar Energy Laboratory; 2017.
31. Hazami M, Naili N, Attar I, Farhat A. Solar water heating systems feasibility for domestic requests in Tunisia: Thermal

potential and economic analysis. *Energ Conver Manage*. 2013;76:599-608. https://doi.org/10.1016/j.enconman.2013.07.079

32. Hazami M, Kooli S, Lazâar M, Farhat A, Belghith A. Energetic and exergetic performances of an economical and available integrated solar storage collector based on concrete matrix. *Energ Conver Manage*. 2010;51(6):1210-1218. https://doi.org/10.1016/j.enconman.2009.12.032

**How to cite this article:** Messaouda A, Hazami M, Mehdaoui F, et al. Thermal performance study of a vacuum integrated solar storage collector (ISSC) with compound parabolic concentrator (CPC). *Int J Energy Res*. 2020;44:756–770. https://doi.org/10.1002/er.4832